Regenerative Therapy 22 (2023) 148–159

Contents lists available at ScienceDirect

Regenerative Therapy

journal homepage: http://www.elsevier.com/locate/reth

Original Article

METTL3 promotes SMSCs chondrogenic differentiation by targeting the MMP3, MMP13, and GATA3

Bin Hu [a], Xiangjie Zou [b], Yaohui Yu [a], Yiqiu Jiang [a, *], Hongyao Xu [a, *]

[a] Department of Sports Medicine and Joint Surgery, Nanjing First Hospital, Nanjing Medical University, Nanjing, China
[b] Department of Orthopedics, Jiangsu Province Hospital, The First Affiliated Hospital of Nanjing Medical University, Nanjing, China

ARTICLE INFO

Article history:
Received 13 December 2022
Received in revised form
9 January 2023
Accepted 14 January 2023

Keywords:
SMSCs
N^6-methyladenosine
Chondrogenesis
METTL3
MeRIP-sequencing

ABSTRACT

Objective: Synovium-derived mesenchymal stem cells (SMSCs) are multipotential non-hematopoietic progenitor cells that can differentiate into various mesenchymal lineages in adipose and bone tissue, especially in chondrogenesis. Post-transcriptional methylation modifications are relative to the various biological development procedures. N^6-methyladenosine (m^6A) methylation has been identified as one of the abundant widespread post-transcriptional modifications. However, the connection between the SMSCs differentiation and m^6A methylation remains unknown and needs further exploration.

Methods: SMSCs were derived from synovial tissues of the knee joint of male Sprague–Dawley (SD) rats. In the chondrogenesis of SMSCs, m^6A regulators were detected by quantitative real-time PCR (RT-PCR) and Western blot (WB). We observed the situation that the knockdown of m^6A "writer" protein methyltransferase-like (METTL)3 in the chondrogenesis of SMSCs. We also mapped the transcript-wide m^6A landscape in chondrogenic differentiation of SMSCs and combined RNA-seq and MeRIP-seq in SMSCs by the interference of METTL3.

Results: The expression of m^6A regulators were regulated in the chondrogenesis of SMSCs, only METTL3 is the most significant factor. In addition, after the knockdown of METTL3, MeRIP-seq and RNA-seq technology were applied to analyze the transcriptome level in SMSCs. 832 DEGs displayed significant changes, consisting of 438 upregulated genes and 394 downregulated genes. DEGs were enriched in signaling pathways regulating the glycosaminoglycan biosynthesis-chondroitin sulfate/dermatan sulfate and ECM-receptor interaction via Kyoto Encyclopedia of genes and genomes (KEGG) pathway enrichment analysis. The findings of this study indicate a difference in transcripts of MMP3, MMP13, and GATA3 containing consensus m^6A motifs required for methylation by METTL3. Further, the reduction of METTL3 decreased the expression of MMP3, MMP13, and GATA3.

Conclusion: These findings confirm the molecular mechanisms of METTL3-mediated m^6A post-transcriptional change in the modulation of SMSCs differentiating into chondrocytes, thus highlighting the potential therapeutic effect of SMSCs for cartilage regeneration.

1. Introduction

The articular cartilage which covers the bone from the outside plays an important buffer role in preventing excessive impact damage. However, the lack of blood supply and nerve nutrition to the cartilage tissue leads to poor regeneration capacity of cartilage [1,2]. Damage to the articular cartilage often leads to joint pain affecting the quality of patient life. Currently available surgical measures including mosaicplasty or microfracture, can alleviate pain to a certain degree, but cannot produce phenotypically stable and sound functional hyaline-like cartilage tissue [2]. The recent

Abbreviations: SMSCs, synovium-derived mesenchymal stem cells; SOX9, SRP (sex determining region Y)-box 9; m^6A, N^6-methyladenosine; COL2A1, collagen type II: alpha 1; METTL3, methyltransferase like 3; MMP3, matrix metallopeptidase 3; MMP13, matrix metallopeptidase 13; GATA3, GATA binding protein 3.

* Corresponding authors. Department of Sports Medicine and Joint Surgery, Nanjing First Hospital, Nanjing Medical University, Nanjing, China
E-mail addresses: JYQ-3000@outlook.com (Y. Jiang), xuhongyao1027@sina.com (H. Xu).

Peer review under responsibility of the Japanese Society for Regenerative Medicine.

https://doi.org/10.1016/j.reth.2023.01.005

advancements in medical science, tissue engineering, and regenerative medicine have resulted in an appropriate biological assay system for cartilage reconstruction. Consequently, the MSCs were selected as suitable seed cells because of their vital potential to be induced into cartilage, bone, and tendon tissue both *in vivo* and *in vitro* [3]. Mesenchymal stem cells have been extracted from the synovial membranes, placenta, bone marrow, and adipose tissue. They are widely applied in regenerative medicine as seed cell resources for tissue repair [4].

There are numerous studies on bone marrow-derived MSCs (BMSCs), however it is challenging to attain BMSCs from bone marrow tissue. Their quantity is usually limited which restricts the widespread use of BMSC in the tissue engineering and regenerative medicine. The SMSCs could also be collected from the synovium of joints, a rich source showing the stem cell characteristics [1]. MSCs extracted from the synovium of joints are suitable for treating the cartilage defects as SMSCs have strong proliferative ability [5] and chondrogenic potential [6]. In addition, synovium tissue isolated from synovial chondromatosis and osteochondral spurs in osteoarthritis (OA) can engender hyaline cartilage under benign conditions, highlighting SMSCs as resources of seed cells for the treatment of articular cartilage defects [7]. Ozeki et al. [8] established a meniscus lesion model with pigs to explore the efficiency of SMSCs for meniscus repair. Thus, the current data suggest the potential of SMSCs in the bone and cartilage disease [9].

Over the past few decades, numerous studies have confirmed that various signaling pathways are involved in the proliferation and differentiation of SMSCs into chondrocytes, including the TGF-β pathway [10], Wnt/β-catenin pathway, Smad, and p38 signal pathway [11]. However, there are large numbers of biological molecules and signaling pathways that affect the chondrogenic differentiation of SMSCs. Therefore, exploring the mechanisms underlying the chondrogenic differentiation of SMSCs is of significant importance.

The previous studies showed that the post-transcriptional modifications in RNA control the expression of genes. N^6-methyladenosine (m^6A) modification is the most general chemical signature in the eukaryotic mRNAs. The dynamic regulation of m^6A modification affects more than 7000 mRNAs in distinctive transcriptomes of mammal cells [12]. RNA modifications, especially N^6-methyladenosine RNA methylation, have been demonstrated to have a vital role in different biological processes, including stem cell renewal, development, tissue homeostasis, and disease progression [13]. MeRIP-seq, as the detection method of m^6A modification, has the presence of detecting m^6A in the whole genome. It can identify the modification level of each gene and compare the advantages between groups [14]. The enrichment and influence of m^6A on RNA are depended on the dynamic interaction between its methyltransferases ("writers"), demethylases ("erasers"), and binding proteins ("readers") [15]. Meanwhile, m^6A modification is regulated by m^6A methyltransferase (METTL3/14, WTAP, ZC3H13, and KIAA1429) [16,17], demethylases (FTO and ALKBH5), and binding proteins (YTHDF1/2/3 AND YTHDC1/2) [18,19]. Methyltransferase-LIKE-3 (METTL3, also known as MT-A70) has been considered the major m^6A-forming enzyme in polyadenylated mRNA [18,19]. METTL3 has been proven to exert pivotal roles in cell differentiation and other important processes [20]. For instance, METTL3 promotes BMCS osteogenic migration and differentiation by facilitating M1 macrophage differentiation [21]. Moreover, METTL3 targets AKT expression by m^6A modification to inhibit MSC adipogenesis [22]. However, it remains unclear whether METTL3 participates in the chondrogenesis of SMCSs.

In the current research, we showed that the m^6A methyltransferases METTL3 has a positive function in increasing the chondrogenic ability of SMCSs by targeting and promoting the expression MMP3, MMP13, and GATA3. Together, our research explored the function of m^6A in the chondrogenic differentiation of SMCSs and revealed different aspects of the new mechanisms participating in the chondrogenic differentiation of SMCSs. Thus, proposing a possible strategy for increasing the efficiency of SMCSs - mediated treatment for cartilage defects.

2. Materials and methods

2.1. Ethical approval

Eight male Sprague Dawley® rats (six to eight-weeks old) of healthy strains were purchased from Nanjing First Hospital (Nanjing, China). The animals were housed at temperature 22 ± 1 °C, relative humidity of 50 ± 1%, and light/dark cycles of 12 h. All animal studies including the mice euthanasia procedure were complied with the regulations and guidelines of Nanjing Medical University Institutional animal care and were performed according to the AAALAC and the IACUC guidelines. The study protocol (DWSY-2104487) was approved by the Experimental Animal Ethics committee of Nanjing Medical University, China.

2.2. SMSCs isolation

SMSCs were derived from the synovial tissues of the knee joint from four male SD rats. The synovium of infrapatellar fat pads was obtained from eight male SD rats. The proliferative synovial tissues of SD rats were cut under aseptic operation. Digestion was terminated using DMEM/F12 complete medium containing 10% fetal bovine serum and 1% double antibody at low temperature and washed with PBS in the super-clean worktable 3 times. Then, 1% type I collagenase (Thermo Fisher, China) was added to 1–2 mm^3-sized synovial fragments. The cells were digested in CO_2 (37.5 °C) incubator for 4 h, after which they were filtered through 120 mesh nylon net (70 μm) and collected. Next, they were cultured with DMEM in a CO_2 incubator at 37.5 °C for 24 h and purified by the optimal density inoculation single clone method. In the next step, 10^3, 10^4, 10^5, and 10^6 cells were spread in the Petri dish of 60 cm^2 and cultured for 14 days. The growth and morphological characteristics of the SMSCs were inspected by an inverted microscope. The clones with appropriate density were selected for separate amplification and culture, and the primary synovial mesenchymal stem cells were obtained. The medium was changed every three days.

2.3. Cell transfection

Lipofectamine 3000 was used to perform transfection. SMCSs were transfected by siRNA against rat METTL3. The following siRNA sequences were synthesized by GENERAL Biosystems Corporation (Anhui, China): shControl 5′-UUCUCCGAACGUGUCACGUTT-3′, shMETTL3 5′UUGCUCUGCUGUUCCUUAGTT 3′. SMSCs (passaged two times) were added to the 6-well plate (1.2×10^5 cells/well) and cultured overnight. Transfection was carried out the next day (e.g., one well was used and two 1.5 ml EP tubes were taken out, one of which was filled with 100 μl opti MEM + 3 μl Lipofectamine 3000, while the other was filled with 100 μl opti MEM + 5 μl siRNA). After mixing, it was placed at room temperature for 15 min and cultured at 37 °C. The cells were collected after 72 h.

2.4. Trilineage differentiation of SMSCs

SMSCs isolated (self-extracted) from SD synovium were placed in 60 cm^2 dishes and cultivated in a chondrogenic, osteogenic, adipogenic medium for 28 days. Later, the $5*10^5$ cells were

centrifuged using 15 ml centrifuge tube and supernatant was discarded. These three-lineage differentiations are as follows:

Chondrogenic differentiation: For chondrogenic induction, cells were cultured in chondrogenic differentiated DMEM (#11965118; Gibco) culture medium 81–7), 1% insulin-transferrin-selenium-sodium pyruvate solution (ITS-A) (#51300044; Gibco). 0.1% proline (#147-85-3; Sigma-Aldrich) and 1% TGF-β3 (#RP8600; Invitrogen). 28 days later, cell samples were harvested for toluidine blue staining. After fixation using 4% paraformaldehyde and embedding in paraffin, tissues sections were stained with toluidine blue (#92-31-9; Sigma-Aldrich) for 30 min.

Osteogenic differentiation: Cells were cultured in basic medium containing 10% FBS, 1% penicillin streptomycin (#15140122; Gibco), 1% glutamine (#56-85-9; Sigma-Aldrich), 0.2% ascorbate, 0.01% dexamethasone, and 1% β-glycerophosphate (#J62121. AD; Thermo Scientific). After 21 days of differentiation, cells were harvested for Alizarin Red staining. Cells were fixed and stained with Alizarin red (#130-22-3; Sigma-Aldrich).

Adipogenic differentiation: Cells were cultured in basic medium containing 10% FBS, 1% penicillin-streptomycin (#15140122; Gibco), 0.1% 1-methyl-3-isobutylxanthine (#28822-58-4; Sigma-Aldrich) 1% glutamine, 0.2% insulin (#11061-68-0; Sigma-Aldrich), 0.2% indomethacin, and 0.1% dexamethasone. Cells were cultured in an induction medium every three days for 28 days for adipogenic differentiation. After 28 days, cells were fixed, rinsed and stained with Oil Red O (#1320-06-5; Sigma-Aldrich).

2.5. Quantitative real-time PCR

SMSCs total RNA was extracted with Trizol reagent (Takara, Dalian, China). A PrimeScript RT kit (Takara, Dalian, China) and the SYBR Premix Ex Taq ™ (Tianjin Southeast Yicheng Technology, China) were applied to amplify relative genes, and an endogenous control β-actin was used by qPCR. The relative gene primers and probes applied in qPCR are shown in Table S1. The reaction under 25 °C lasted 5 min; under 42 °C lasted 60 s and under 85 °C lasted 15 s. According to the manufacturer's instructions, RNA m^6A level was detected with m^6A RNA Methylation Quantification Kit (ab185912, Abcam). Next, at a wavelength of 450 nm, the absorbance of each well was quantified. The m^6A levels calculations were performed based on the standard curve.

2.6. Quantification of total m6A levels

According to the manufacturer's instructions, RNA m^6A level was detected with EpiQuik m^6A RNA Methylation Quantification Kit (P-9005, Epigentek). Then, the absorbance of each well was quantified at a wavelength of 450 nm. The m^6A levels calculations were performed based on the standard curve.

2.7. Gene-specific m^6A qPCR

The Imprint® RNA Immunoprecipitation kit (Sigma) was applied for MeRIP. In brief, 5×10^6 SMSCs were purified with RNA Immunoprecipitation (RIP; Abcam, Cambridge, UK) lysis buffer and cultured in RIP buffer containing protein A/G magnetic beads combined with Anti-m^6A antibody (Abcam) overnight at 4 °C. Next, RNAs, which were handled with the immune sedimentation method, were extracted to analyze the levels of m^6A of the relative mRNAs.

2.8. Western blotting

SMSCs were collected on ice with PBS and the Western blot analysis was performed as previously described [21]. All proteins were collected by using lysis buffer and the sample/handled protein (30 μg) was added to SDS-PAGE and shifted on PVDF membranes (Beijing Liuyi Biotechnology, China). Membranes were then incubated with the antibodies against SRY-Box 9 (SOX9; cat.67439-1-Ig, Proteintech), aggrecan (ACAN; cat.13880-1-AP, Proteintech), type II collagen (COL2A1; cat.28459-1-AP, Proteintech), MMP3 (cat.66338-1-Ig, Proteintech), MMP13 (cat.18165-1-AP, Proteintech), GATA3 (cat.66400-1-Ig, Proteintech), and tubulin (cat. 10094-1-AP, Proteintech) at 4 °C overnight; all antibodies were diluted using 1:1000 ratio. Then, the membranes were incubated with secondary antibodies and cultured again for 1 h at 25 °C. The film was placed in super ECL plus hypersensitive luminous solution for 2 min, after which the densitometry was graphed using image J (Version 1.8,0, USA).

2.9. Flow cytometry

The surface markers of the SMSCs were analyzed by utilizing flow cytometric analysis. SMSCs passaged for 2 times were harvested and washed in PBS. SMSCs (1.0×10^6) were then incubated with CD73 antibody (cat.12231-1-AP; 1:500 dilution, Proteintech), CD45 antibody (cat. 60287-1-Ig; 1:500 dilution, Proteintech), CD44 antibody (cat.12231-1-AP; 1:500 dilution, Proteintech), CD90 antibody (cat. 65088-1-Ig; 1:500 dilution, Proteintech), and CD105 antibody (cat. 10862-1-AP; 1:500 dilution, Proteintech) for at last 90 min at 37 °C and analyzed using flow cytometry.

2.10. MeRIP-sequencing and RNA-sequencing

In SMSCs, siRNA was designed to reduce the expression of METTL3 and culture with a chondrogenic culture medium for 28 days. The RNAs of SMSCs were refined with TRIzol reagent (Takara, Dalian, China), after which we used poly-T oligo attached magnetic beads (Invitrogen, CA, USA) to extract about 100 μg of RNA from poly(A) mRNA. Then, BSA (0.5 $\mu g\ \mu l^{-1}$) was added to the lysed RNA fragmentation. Eluted m6A-containing fragments and untreated inputs control fragments were converted to the final cDNA library in accordance with strand-specific library preparation by the dUTP method. Finally, we performed 2×150 bp paired-end sequencing analyses on the Illumina Novaseq ™ 6000 platform according to the method recommended by the supplier.

2.11. GO and KEGG analysis

GO enrichment and KEGG pathway enrichment analysis of peaks and differential peaks were performed using R based on the hypergeometric distribution. A $p < 0.05$ denoted the significance of GO term enrichment. Pathway analysis was performed based on the KEGG database to investigate the potential functions. The GO and pathway enrichment analysis were also performed based on the differentially regulated m6A peaks and mRNAs. The ggplot 2 was used for graphing and data visualization.

2.12. Statistical analysis

Numerical data are presented as mean ± standard deviation (Std). Statistical tests in this experiment were performed using GraphPad Prism version 7.01 (GraphPad Software, San Diego, CA). Student t-test was used to analyze the significant difference between two groups. A p value < 0.05 was considered to be statistically significant.

3. Results

3.1. Complete induction of chondrogenic differentiation of SMSCs

All SMSCs were of fusiform shape. To prove the multi-differential potential of the isolated SMSCs, we incubated the SMSCs with an osteogenic, adipogenic, and chondrogenic medium. The results of the histological analysis including ARS staining and Oil Red O staining are shown in Fig. 1A. Flow cytometry was applied to analyze the surface-specific proteins of SMSCs; CD44, CD73, CD90, and CD105 were expressed in SMSCs, while CD45 was not detected (Fig. 1B). When cultured in a chondrogenic medium for 28 d, the SMSCs could be induced to differentiate along with the chondrogenic way. The chondrogenic potency of SMSCs, cultured with or without a chondrogenic medium, was demonstrated by staining cells with sulfated glycosaminoglycans using Safranin-O and Toluidine Blue (Fig. 1C). Next, we confirmed that the gene levels of chondrogenic differentiation markers SOX9, ACAN, and COL2A1 were higher in the induction (28 d) group than in the control groups (Fig. 1D). The three proteins were also detected by WB, which was consistent with the above PCR results (Fig. 1E). Thus, these data suggested that SMSCs had the characteristics of MSCs and could be successfully induced into chondrocytes.

3.2. METTL3 and m^{6}A modification are increased in chondrogenic differentiation

In chondrogenic differentiation, we detected the content of m6A to identify the potential role of m6A modification. Compared with the non-induced SMSCs, the m^{6}A level of m^{6}A in SMSCs was higher than 28 d-induced SMSCs ($p < 0.05$, Fig. 2A). Based on the previous experiment [22,23], m^{6}A post-transcriptional modifications markedly affected many aspects as they were dynamically regulated by m^{6}A methyltransferase and m^{6}A demethylase. Next, we detected the mRNA content of m^{6}A modified molecules, consisting of (methyltransferase) METTL3, METTL14, WTAP, KIAA1429, and ZC3H13 (demethyltransferase) FTO, and ALKBH5. In the induction group, METTL3 and METTL14 were significantly increased compared to the control group ($p < 0.05$). Nevertheless, the other genes (WTAP, FTO, ALKBH5, KIAA1429, and ZC3H13) revealed no noticeable changes between the induction group and control group (all $p < 0.05$, Fig. 2B). In addition, Western blotting indicated that protein levels METTL3 were most obviously upregulated in the chondrogenic potential of SMSCs (Fig. 2C). Hence, we assumed that METTL3 was a pivotal regulator that resulted in the m^{6}A modifications of the chondrogenic differentiation. Then, METTL3 was chosen for further experiments.

3.3. METTL3 knockdown suppresses chondrogenic differentiation

In order to explore the effect of m^{6}A in the chondrogenic differentiation procedure of SMSCs, the METTL3 was chosen to perform siRNA transfection experiments. We designed three siRNA (METTL3-sh1, METTL3-sh2, METTL3-sh3), where Mettl3-sh3 knockdown results from WB were the most significant (Fig. 3A). Thus, METTL3-sh3 was chosen for further experiments, and the shRNAs were used to interfere with the expression of METTL3 in SMSCs. Then, the quantification of transfer efficiency in SMSCs was computed through the proportion of fluorocytes. METTL3 silencing efficiency of approximately 80% was acquired at 48 h after interfering (Fig. 3A). WB was used to detect METTL3 protein levels. Compared with the SMSCs, it showed a significant decline in the shMETTL3 group ($p < 0.05$), which revealed that METTL3 was significantly knockdown in SMSCs (Fig. 3A).

To explore the chondrogenic potential of SMSCs between the shMETTL3 group and shControl group, Safranin-O, and Toluidine blue was used for staining sulfated glycosaminoglycans. Grossly, shControl-induction group pellets were rounder and larger than shMETTL3-induction group pellets (Fig. 3B).

Next, the expression level of three chondrocytes-specific markers was detected. The qRT-PCR exhibited a sharp decline in the mRNA level of SOX9, ACAN, and COL2A1 in SMSCs after culturing with a chondrogenic medium for 28 days (Fig. 3C). The results of WB of SOX9, ACAN, and COL2A1 showed the same trend (Fig. 3D), which suggested that the effect of METTL3 was essential during the chondrogenic differentiation process of SMSCs.

3.4. Transcriptome-wide m^{6}A methylome during chondrogenic differentiation of SMSCs

In chondrogenesis of SMSCs, m^{6}A peaks were relatively unusual. Therefore, to analyze the potential function of m^{6}A during the chondrogenesis of SMSCs, we used the MeRIP-Seq to map the pivotal landscape of the m^{6}A methylome. With reference to shControl-Control, shControl-induction, shMETTL3-Control, and shMETTL3-induction, 38.47%, 38.61%, 39.85%, 38.31% of the peaks were located in the 3′untranslated (UTR) region, 14%、14.74%、13.58%、13.74% of the peaks were located in the 5′untranslated (UTR) region, and 5.15%、5.28%、5.17%、5.11% in the first exon, and 42.38%、41.37%、41.4%、42.83% in the other exons, respectively (Fig. S1 a-d). SMSCs (shControl, shMETTL3) m^{6}A peak density of mRNAs was further dissected through the MeRIP-Seq. These m^{6}A modifications were mainly detected in the coding sequence and the 3′-UTR (Fig. 4A). In addition, the motif analysis proved that m^{6}A RRACH (R was purine, A was m^{6}A, and H was a non-guanine base) consensus sequence enrichment between shControl and shMETTL3 (Fig. 4B). According to the criterion of fold change (FC) $\geq$ 1.5, $p < 0.05$, 1319 m^{6}A peaks were detected after a 28-day of chondrogenic induction of SMSCs (shControl-induction). In addition, 708 hyper-methylated m^{6}A peaks and 611 hypo-methylated m^{6}A peaks were discovered (Fig. 4C and Table S2). To explore the biological function of m^{6}A methylation in the chondrogenic of SMSCs, GO and KEGG pathway analysis of DMGs were analyzed. GO analysis discovered that the DMGs between shControl-Control and shControl-induction were predominantly related to (ontology: biological process) “regulation of transcription by RNA polymerase II especially by acting as a regulator of chondrocyte phenotype” “microtubule-based movement especially more extensive movement”; (ontology: cellular component) “membrane,” nucleus,” and “cytoplasm”; and (ontology: molecular function) “ATP binding,” “nucleic acid binding” and “DNA binding” (Fig. 4D). Moreover, KEGG pathway analysis revealed that the DMGs were strongly correlated with the signaling pathway” phosphatidylinositol signaling system,” “RNA degradation,” and “mRNA surveillance pathway" (Fig. 4E). We inferred that transcriptome-wide m^{6}A methylome occurred during chondrogenic differentiation of SMSCs.

3.5. The combination of MeRIP-Seq and RNA-seq indication of METTL3 downstream targets

As METTL3 is involved with chondrogenic differentiation of SMSCs via m^{6}A demethylation activity, MeRIP-sequencing was applied to analyze the shControl-induction SMSCs and shMETTL3-induction SMSCs. In addition, compared with the shControl-induction group, abnormal peaks were found in the 3′UTR region with a 35.74% proportion, 15.4% in the 5′UTR region, and 6.76% in the first exon, and 42.09% in the other exons (Fig. 5A). In addition, after the knockdown of METTL3, RNA-seq technology was applied to analyze differential gene expression (DEGs) at the transcriptome

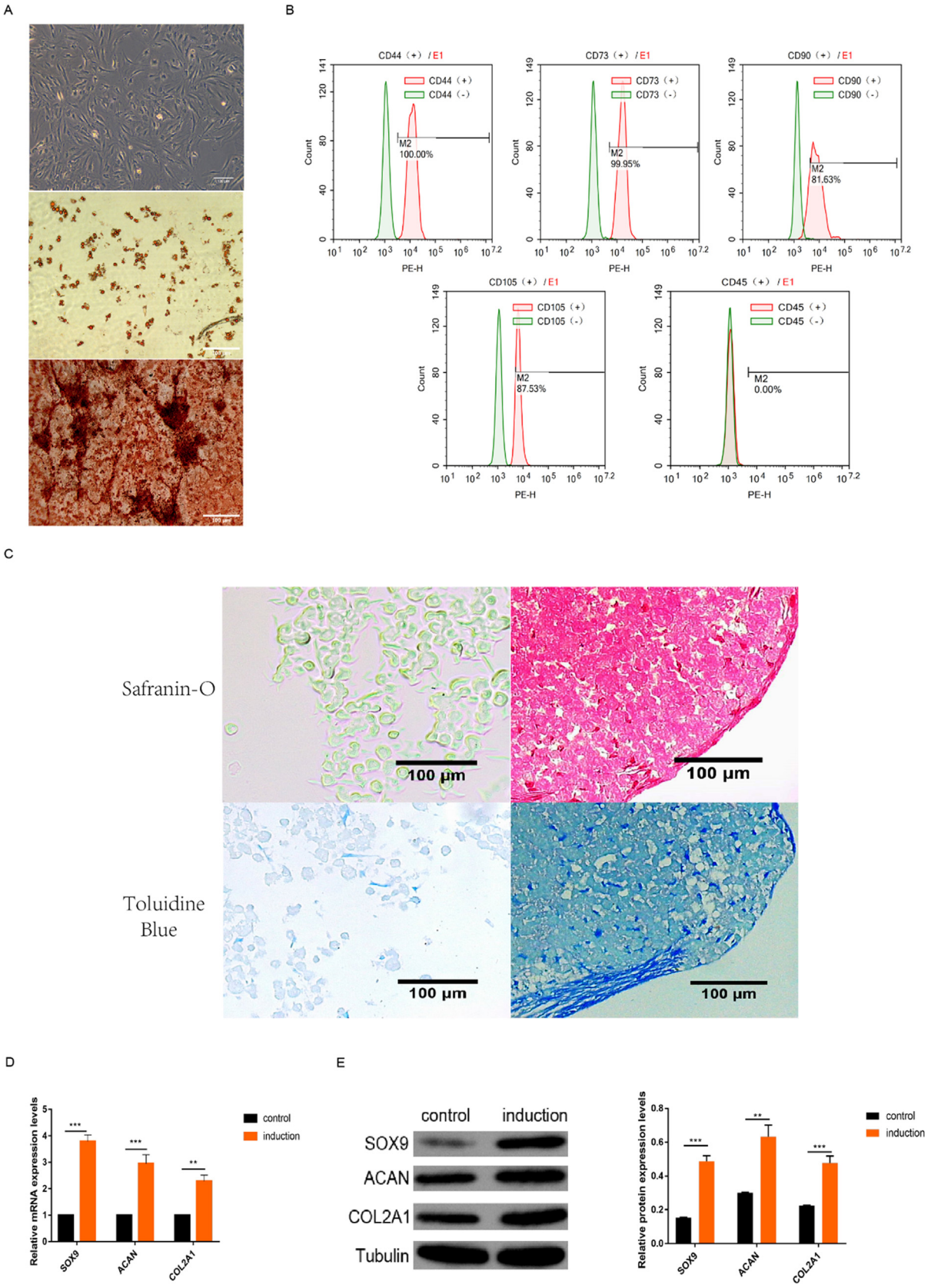

Fig. 1. *In vitro* differentiation of SMSCs. (A) All SMSCs were of fusiform shape. Oil red O staining was performed to confirm adipogenesis and osteogenesis via alizarin red S staining (ARS). Scale bars, 100 μm. **(B)** Surface marker expression of SMSCs. **(C)** The chondrogenic potential was confirmed by using Safranin-O and Toluidine Blue. Scale bars, 100 μm. **(D)** qRT-PCR analysis of chondrogenic genes (SOX9, ACAN, and COL2A1) during the chondrogenic differentiation of SMSCs (28 d). **(E)** Western blot analysis and quantitative protein expression of SOX9, ACAN, and COL2A1 at 28 d of SMSCs chondrogenic differentiation. The Western blot analysis revealed that the target protein levels were quantified by densitometry and normalized to tubulin. All results are presented as mean values ± SEM; n = 3; (*$p < 0.05$, **$p < 0.01$, ***$p < 0.001$), compared with the control groups.

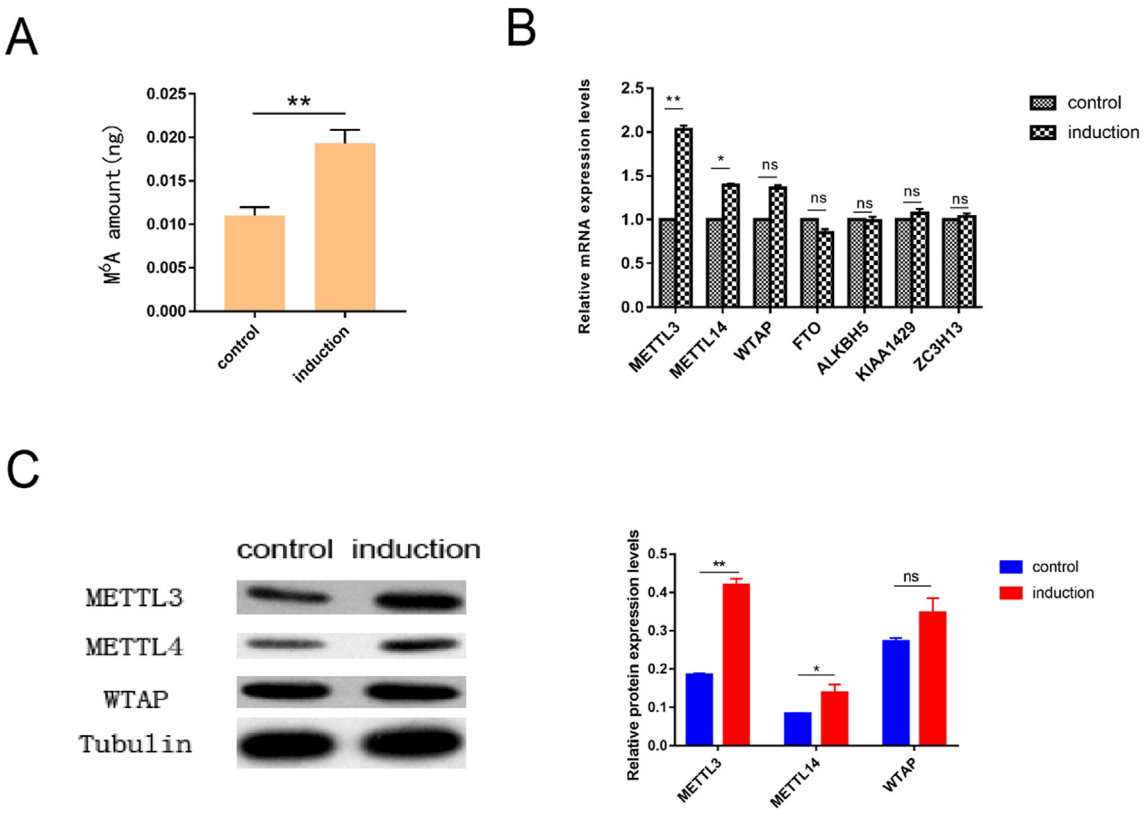

Fig. 2. METTL3 contributes to the abnormal m^{6}A modification in chondrogenic differentiation. (A) The m^{6}A levels in SMSCs RNA of chondrogenic differentiation. **(B)** mRNA content of relevant m^{6}A modified genes in chondrogenic differentiation. **(C)** The Western blotting analyzed the protein content of METTL3, METTL14, and WTAP in the induced group and control SMSCs. All results are presented as mean values ± SEM; n = 3; (*$p < 0.05$, **$p < 0.01$, ***$p < 0.001$), compared with the control groups.

level in SMSCs. 832 DEGs displayed significant changes, consisting of 438 upregulated genes and 394 downregulated genes (Fig. 5B and Table S3). DEGs were enriched in the signaling pathways regulating the glycosaminoglycan biosynthesis chondroitin sulfate/dermatan sulfate and ECM-receptor interaction via Kyoto Encyclopedia of Genes and Genomes (KEGG) pathway enrichment analysis (Fig. 5C). Gene Ontology (GO) annotations of these DEGs were associated with "cell adhesion molecule binding," "3′,5'−cyclic−AMP phosphodiesterase activity", and "extracellular matrix binding" (Fig. 5D). These results revealed that METTL3 has a pivotal function during the chondrogenic differentiation of SMSCs. MMPs are remodeling enzymes involved in tissue development and elevated expression is deleterious in adult cartilage. GATA3, a transcript factor, is downregulated in osteosarcoma and precipitates Epithelial−mesenchymal transition (EMT). A closer look at MMPs, particularly transcription factors, would be of interest as a focus discussion point. In consideration of their roles in chondrogenesis, Integrative Genomics Viewer (IGV) analysis was used to clarify the peak calling of MMP3, MMP13, and GATA3, revealing that the m^{6}A installed on MMP3, MMP13, and GATA3 and the m^{6}A peak in the shMETTL3-induction SMSCs was lower (Fig. 5E–F). Consequently, we conjectured that MMP3, MMP13, and GATA3 were the targets of METTL3.

3.6. METTL3 upregulates the expression of MMP3, MMP13, and GATA3 through m^{6}A modification

Methylated RNA immunoprecipitation qPCR (MeRIP-qPCR) was applied to determine whether MMP3, MMP13, and GATA3 are regulated by METTL3. m^{6}A-specific antibodies were predominantly located in MMP3, MMP13, and GATA3, consistent with integrative genomics viewer (IGV) software analysis and professional software for visualization of high-throughput sequencing data (Fig. 6A).

It draws a peak calling map for a high-enriched region of a gene[23]. In addition, the qRT-PCR results confirmed that the expression of MMP3, MMP13, and GATA3 in the shMETTL3-induction SMSCs was higher than in the shControl-induction SMSCs ($p < 0.05$, Fig. 6B). Western blotting results also showed that knocking down METTL3 promoted the expression of MMP3, MMP13, and GATA3 (Fig. 6C). This also suggested that these three genes may have an essential role in chondrogenesis. Furthermore, these findings confirmed the reliability of m^{6}A-seq and RNA-seq results. They also indicated that METTL3 regulates the expression of MMP3, MMP13, and GATA3.

4. Discussion

SMCSs share specific characteristics with mesenchymal stem cells with many available resources and the advantage of chondrogenesis, which have been fascinating for regenerative medicine and tissue engineering. Several reports have demonstrated that m^{6}A modification and METTL3 have a pivotal function in determining the purpose of stem cells and early embryonic progress in mammals [23,24]. However, the function of METTL3 and m^{6}A in the chondrogenic differentiation of SMSCs remain unclear.

We isolated and cultured the rat synovial mesenchymal stem cells in the present study. In order to characterize SMSCs, we detected with SMSCs surface markers. After incubation in a chondrogenic medium for 28 d, SMSCs were successfully induced into chondrocytes. In addition, we identified the pivotal role of METTL3 during the chondrogenic differentiation of SMCSs, which is conducive to investigating the mechanism of chondrogenic

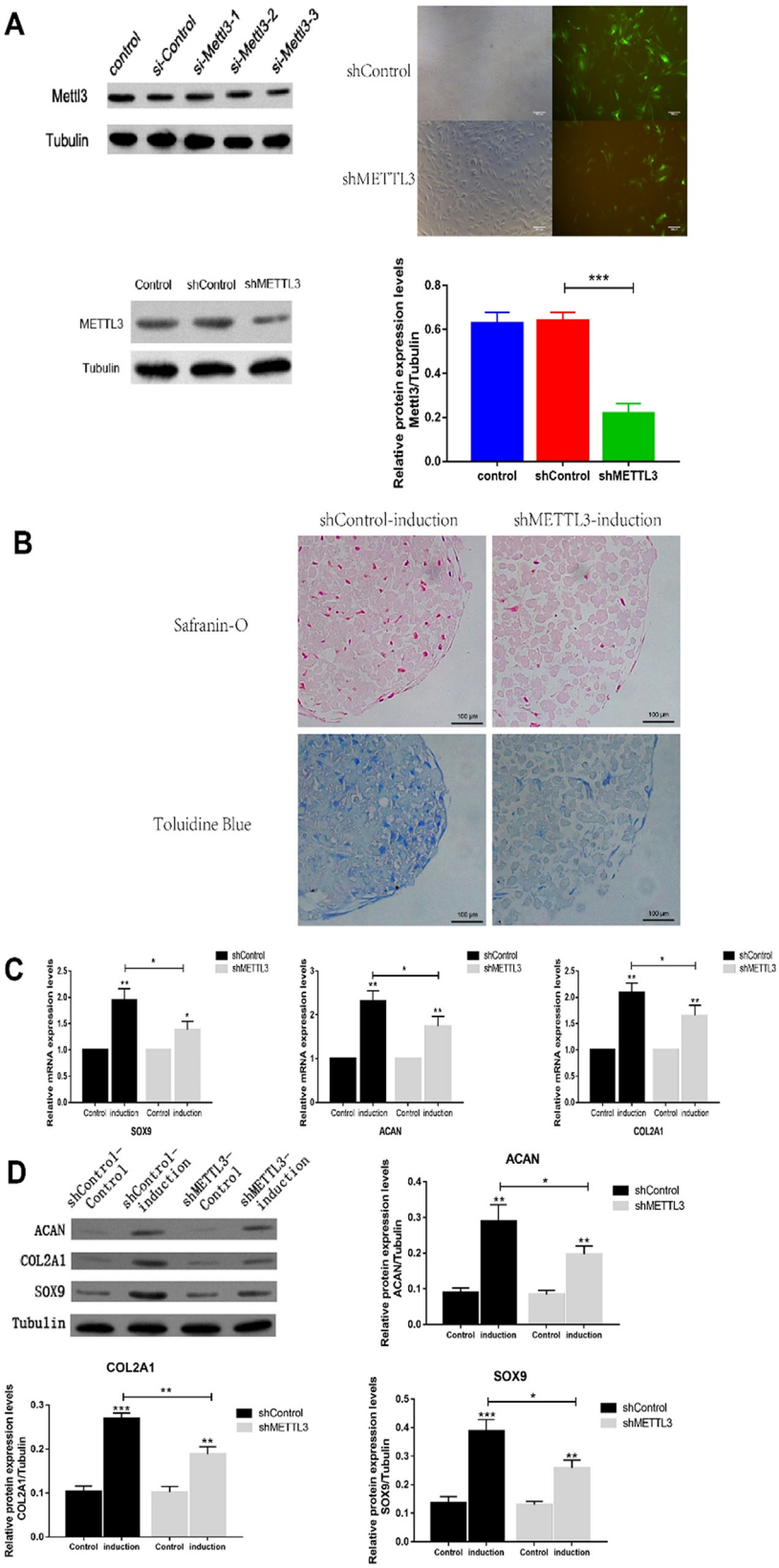

Fig. 3. The knockdown METTL3 inhibited chondrogenic differentiation of SMSCs. (A) After transfection for 72 h, Fluorescence protein marker and WB were applied to detect the transfer efficiency of interfering METTL3 in SMSCs. Scale bars, 100 μm. **(B)** SMSCs culture of Safranin-O and Toluidine blue staining was performed at 28 d, before and after induction, respectively, during differentiation. Scale bars, 100 100 μm. **(C)** The mRNA expression levels of SOX9, ACAN, and COL2A1 in the shMETTL3-induction and shControl-induction groups were detected by qRT-PCR after 28 days of incubation, with β-actin acting as an internal control. **(D)** The Western blotting was utilized to detect the relative protein expression content in the shMETTL3-induction and shControl-induction groups. Tubulin was used as an internal control. All results are presented as mean value s± SEM; n = 3; (*$p < 0.05$, **$p < 0.01$, ***$p < 0.001$) compared with the control groups.

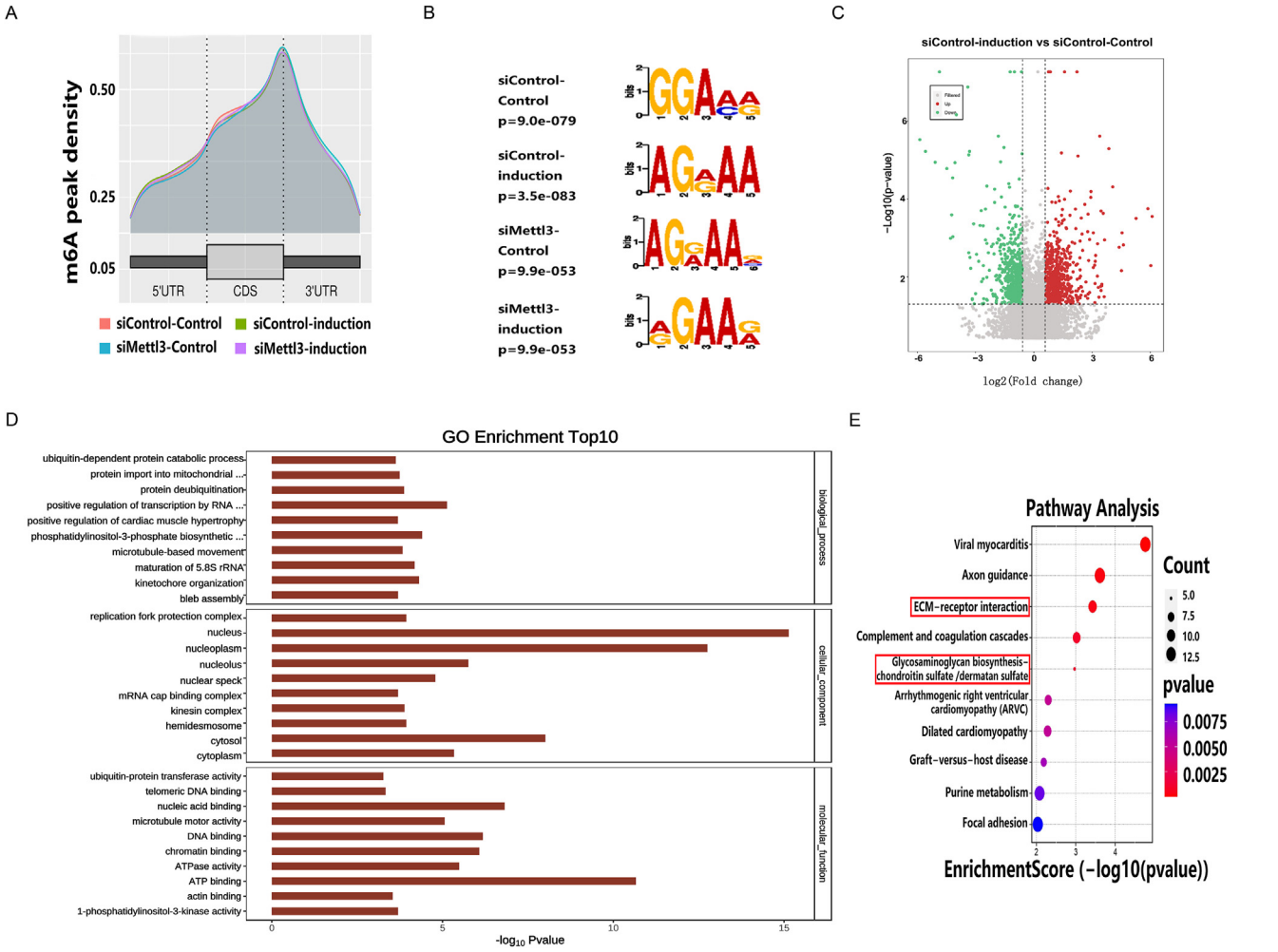

Fig. 4. m6A methylation profile during chondrogenic differentiation of SMCSs. (A) The m^{6}A motifs predominantly located across m^{6}A peaks were detected between the shControl (Control, induction) group and the shMETTL3 (Control, induction) group. **(B)** Density distribution of m^{6}A peaks across mRNA transcripts in the shControl (Control, induction) group and shMETTL3 (Control, induction) group. **(C)** A Volcano plot MeRIP-Seq showed the expression DMGs. **(D)** Differentially methylated genes GO enrichment. **(E)** Differentially methylated genes KEGG enrichment (fold change $\geq$ 1.5, $p < 0.05$).

differentiation. With the technology of RNA-seq and MeRIP-Seq, we mapped the transcriptome-wide m^{6}A methylome, finding the METTL3 downstream regulatory genes (MMP3, MMP13, and GATA3) in the procedure of chondrogenic differentiation of SMSCs.

Recently, m^{6}A has been identified as a dynamic adjustment process, installed by “writers” (METTL3, METTL14 AND WTAP), removed by “easers” (ALKBH5 and FTO), and recognized by “readers” (YTHDF1, YTHDF2, and YTHDF3) [20]. N6-methyladenosine (m6A) modification is essential for participation in various biological processes. Therefore, more attention was paid to m^{6}A regulation in MCSs. METTL3-mediated m^{6}A RNA methylation is essential in bone marrow mesenchymal stem cells during osteogenic differentiation [25]. BMSCs isolated from AML (acute myeloid leukemia) patients were found to have increased adipogenesis, and METTL3 significantly inhibited human BMSC adipogenesis [22]. Liang et al., also studied METTL3 as part of their research which demonstrated that the Notch signaling pathway is a key downstream target of the modulation of muscle stem cells [25,26]. These data suggested that the METTL3-mediated m^{6}A modification facilitated the differentiation of MCSs.

In order to investigate whether the METTL3-mediated m^{6}A modification was involved in the chondrogenesis of SMCSs, we first found that the content of m^{6}A of SMCSs was significantly increased after chondrogenesis. Then, to explore this change, we measured several enzymes essential for m^{6}A methylation, methyltransferases (METTL3, METTL14, WTAP, ZC3H13, AND KIAA1429), and demethylases (FTO and ALKBH5). We found that METTL3 underwent the most significant change among all enzymes, and we speculated that mettl3 had an essential role in chondrogenic differentiation. Inhibition of METTL3 could reduce chondrogenesis of SMCSs, as was shown by using Toluidine blue staining and Safranin-O analysis. In addition, we investigated the function of METTL3 on the expression of chondrogenic markers (SOX9, ACAN, and COL2A1), finding that METTL3 knockdown significantly weakened cartilage formation [26,27]. These results revealed that METTL3 developed a pivotal inhibitory function in regulating chondrogenic differentiation. Briefly, the m^{6}A MeRIP-Seq showed enrichment of 2.85 and 2.96 peaks percentage of the genome for the control and induced groups (28 d). Moreover, the m^{6}A enrichment between the control group and induced group (induced , 28 d) was predominantly located in the 3′UTR region and near the stop codon; these sites were m^{6}A-particular and are consistent with the previously published studies [20,28]. In the chondrogenic differentiation of SMSCs, the differentially methylated peaks mainly focused on “regulation of transcription by RNA polymerase II” and “microtubule-based movement” [1], thus suggesting that the m^{6}A has a conservative

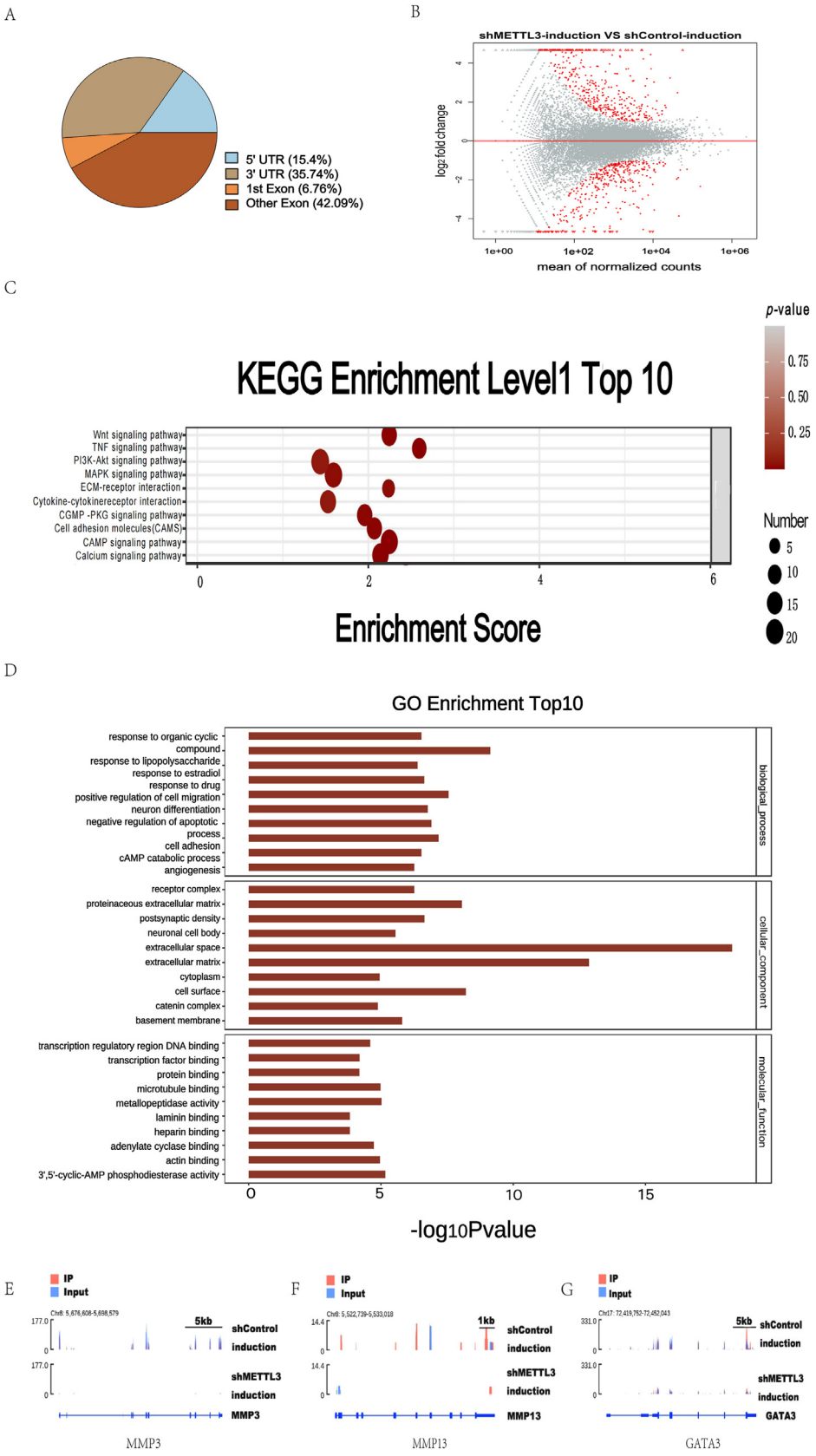

Fig. 5. The combination of MeRIP-Seq and RNA-seq indications of METTL3 downstream targets. (A) The distribution of differentially methylated m^{6}A peaks (shMETTL3-induction vs. shControl-induction) is displayed using a pie chart. **(B)** Volcano plot displaying the DEGs (fold change≥ 1.5, $p < 0.05$). **(C)** Differentially expressed genes KEGG enrichment Level 1 Top 10. **(D)** GO enrichment was used to analyze DEGs. (E–G) IGV software analysis of the m^{6}A modification of MMP3, MMP13, and GATA3.

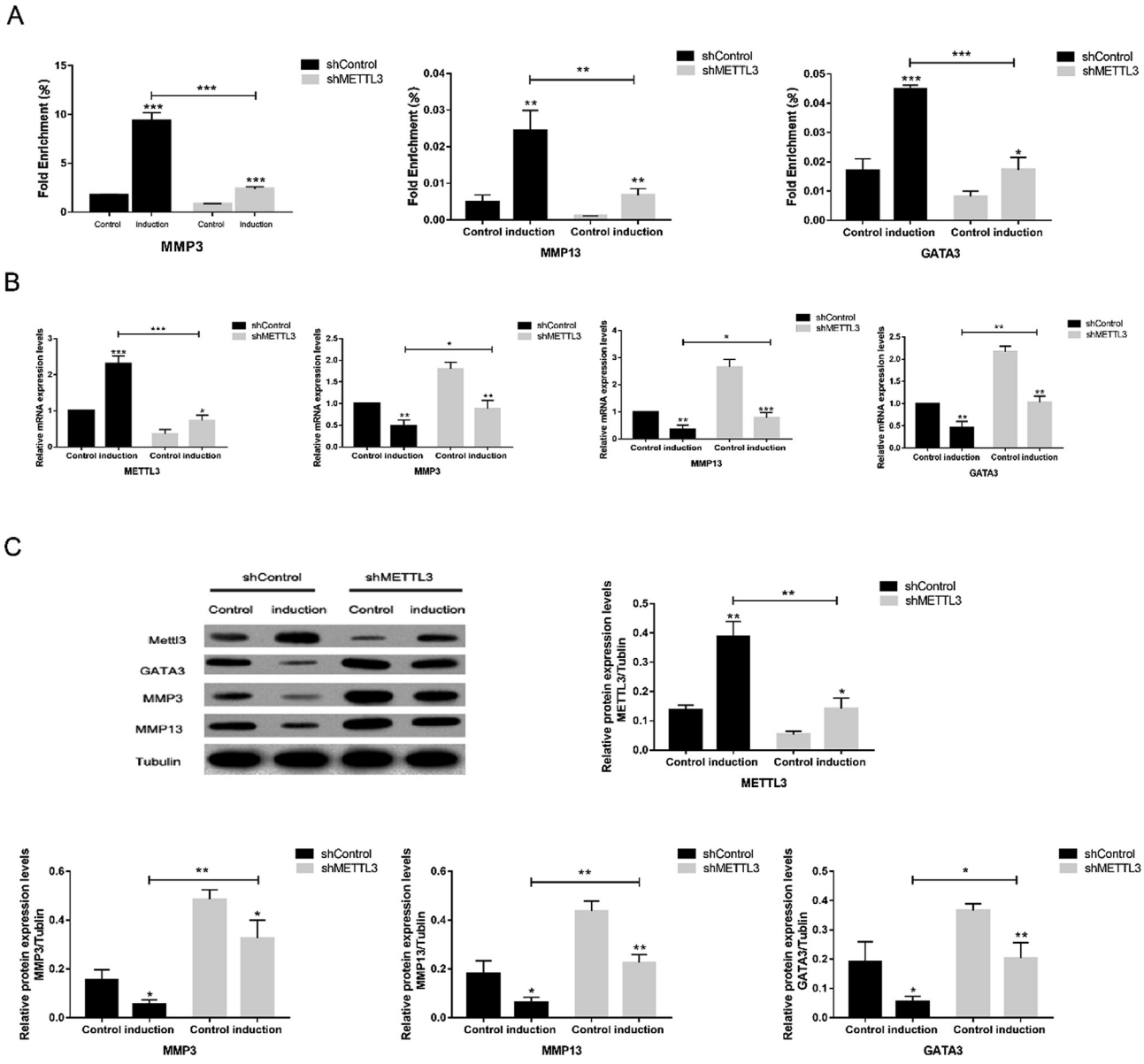

Fig. 6. Analysis of alterations in four representative genes. (A) MeRIP-qPCR analysis of MMP3, MMP13, and GATA3 mRNA in the shControl (Control, induction) and shMETTL3 (Control, induction) SMSCs. **(B)** qRT-PCR results of METTL3, MMP3, MMP13, and GATA3 after interfering with METTL3 expression (Control, induction). **(C)** Western blotting was used to detect and quantify METTL3 MMP3, MMP13, and GATA3 (Control, induction) after interfering with MTTTL3 expression. All results are presented as mean values ± SEM; n = 3; (*$p < 0.05$, **$p < 0.01$, ***$p < 0.001$) compared with the control groups.

and essential role in the regulation of cellular progress and operations. To clarify the role of m^6A in determining chondrogenic differentiation of SMSCs, we combined the technology of RNA-seq with m^6A seq and found the pivotal genes (MMP3、MMP13、GATA3) that were affected by m^6A modification.

Matrix Metalloproteinases (MMPs) are members of zinc-dependent endopeptidases that have an important effect on regulating pathological processes, which they exert in different ways. It has been reported that MMP3 is associated with remodeling extracellular matrix ECM [29] and migration in the MSCs [30]. When cultured in an inflammation-conditioned medium, human MSCs show poor chondrogenic ability with increasing expression of MMP3, MMP13 and reduced gene expression of SOX9, aggrecan, and type II collagen [31]. It has also been demonstrated that MMP-3 is related to angiogenesis in the human adipose-derived mesenchymal stem cells [32]. According to previous studies, the researchers focused their main attention on the function of MMP13 in the osteogenic differentiation of MSCs.

Moreover, hMSCs incubated with Col I matrix can increase the levels of MMP13 and facilitate the osteogenic differentiation of hMSCs [32,33]. In brief, MMP13 has an essential function in bone biology because of its unique role in the degradation of the extracellular matrix and the progression of osteoarthritis [34], particularly the collagens [35]. This study found an association between the m6A methylation and MMP3, MMP13, and GATA3 in SMSCs' chondrogenic differentiation. The previous study demonstrated that the m6A methylation on the 3' UTR of GATA3 pre-mRNA leads to the separation of the RNA-binding protein HuR and the degradation of GATA3 pre-mRNA, suggesting its association [36].

GATA-3 has a zinc finger domain, which is closely correlated to the DNA-binding domain of the erythroid-specific transcription factor [37]. It can be involved in autophagy by binding to the

promoter of Cellular Repressor of E1A-stimulated Genes (CREG) and increasing the levels of CREG expression in BMSCs [37,38]. In osteosarcoma, GATA3 has lower expression than in paracarcinoma tissue, while levels of GATA3 are connected with osteosarcoma cell migration and metastasis [37,38]. In addition, GATA-3 is involved in luminal epithelial differentiation by binding to the FOXA1 promoter in the mammary gland [39]. It is also expressed during the human later skin development period, while its central role in fetal human skin development has been well-documented [40]. According to our observation, the expression of GATA3 decreased during chondrogenesis. We speculated that GATA3 has a negative effect on the chondrogenesis of SMSCs. However, its specific role in synovial mesenchymal stem cells is still unclear. The present study found that MMP3, MMP13, and GATA3 were differentially expressed by using RNA-seq technology. Through IGV software, we explored the changes in m6A levels of these three genes and found abnormal peaks caused by METTL3, thus suggesting that m6A may be involved in the degradation of MMP3, MMP13, and GATA3.

This study demonstrated that the alteration of m^6A methylation in the chondrogenesis of SMSCs. The combination of RNA-seq and MeRIP-seq were used to map the transcript-wide m^6A landscape. MMP3, MMP13 and GATA3 can be used as potential therapeutic targets. Altogether, our data showed a fundamental contribution for further research aiming to find a novel therapeutic targets for difficulty in chondrogenesis.

4.1. Limitations

This study also has limitations. (i) The main limitation of this study is that we did not further explore the mechanisms of METTL3 *in vivo.* (ii) We did not observe the knockdown of METTL3 detected in these long-term cultures. (iii) Type II collagen is a secreted protein in the triple-helical assembly. Western blot does not explore much about collagen synthesis as it shows the single subunit. (iv) In this study, we have only considered silencing METLL3 with siRNA but not the mixture of siRNAs; and fold change (1.5) for the volcano plot. However, we plan to consider these in our future studies.

5. Conclusion

Our basic findings suggest that the METTL3-mediated m^6A modification produces a marked regulatory effect during the chondrogenic differentiation processes of SMCSs. Our data revealed that the whole m^6A modification is upregulated in the chondrogenic differentiation of SMCSs. We mapped the landscape of transcriptome-wide m^6A methylome. However, more studies are needed to confirm our findings further. Our results show that the METTL3-mediated m^6A modification by targeting MMP3, MMP13, and GATA3 promotes chondrogenic differentiation of SMCSs.

Data availability

All Seq data have been deposited into Sequence Read Archive database with the identifiifier PRJNA885046.

Declaration of competing interest

The authors report no conflict of interest in this work.

Acknowledgments

This work was supported by Nanjing Municipal Science and Technology Bureau International Joint Research and Development (No.201911041), Jiangsu Province Social development general project (No. SBE2020740551). The Development Funding of Nanjing Health Science and Technology (No. YKK20112).

Appendix A. Supplementary data

Supplementary data to this article can be found online at https://doi.org/10.1016/j.reth.2023.01.005.

References

[1] Li J, Sun Z, Lv Z, Jiang H, Liu A, Wang M, et al. Microtubule stabilization enhances the chondrogenesis of synovial mesenchymal stem cells. Front Cell Dev Biol 2021;9.
[2] Richter DL, Schenck Jr RC, Wascher DC, Treme G. Knee articular cartilage repair and restoration techniques: a review of the literature. Sports health 2016;8(2):153–60.
[3] Charbord P. Bone marrow mesenchymal stem cells: historical overview and concepts. Hum Gene Ther 2010;21(9):1045–56.
[4] Sekiya I, Koga H, Otabe K, Nakagawa Y, Katano H, Ozeki N, et al. Additional use of synovial mesenchymal stem cell transplantation following surgical repair of a complex degenerative tear of the medial meniscus of the knee: a case report. Cell Transplant 2019;28(11):1445–54.
[5] Nimura A, Muneta T, Koga H, Mochizuki T, Suzuki K, Makino H, et al. Increased proliferation of human synovial mesenchymal stem cells with autologous human serum: comparisons with bone marrow mesenchymal stem cells and with fetal bovine serum. Arthritis Rheum: Official J American College of Rheumatol 2008;58(2):501–10.
[6] Sakaguchi Y, Sekiya I, Yagishita K, Muneta T. Comparison of human stem cells derived from various mesenchymal tissues: superiority of synovium as a cell source. Arthritis Rheum: Official Journal of the American College of Rheumatology 2005;52(8):2521–9.
[7] Kim YS, Kim YI, Koh YG. Intra-articular injection of human synovium-derived mesenchymal stem cells in beagles with surgery-induced osteoarthritis. Knee 2021;28:159–68.
[8] Ozeki N, Kohno Y, Kushida Y, Watanabe N, Mizuno M, Katano H, et al. Synovial mesenchymal stem cells promote the meniscus repair in a novel pig meniscus injury model. J Orthop Res 2021;39(1):177–83.
[9] Li N, Gao J, Mi L, Zhang G, Zhang L, Zhang N, et al. Synovial membrane mesenchymal stem cells: past life, current situation, and application in bone and joint diseases. Stem Cell Res Ther 2020;11(1):1–12.
[10] Ham O, Lee CY, Kim R, Lee J, Oh S, Lee MY, et al. Therapeutic potential of differentiated mesenchymal stem cells for treatment of osteoarthritis. Int J Mol Sci 2015;16(7):14961–78.
[11] Henderson SE, Santangelo KS, Bertone AL. Chondrogenic effects of exogenous retinoic acid or a retinoic acid receptor antagonist (LE135) on equine chondrocytes and bone marrow-derived mesenchymal stem cells in monolayer culture. Am J Vet Res 2011;72(7):884–92.
[12] Wu R, Jiang D, Wang Y, Wang X. N 6-methyladenosine (m6A) methylation in mRNA with A dynamic and reversible epigenetic modification. Mol Biotechnol 2016;58(7):450–9.
[13] Batista PJ, Molinie B, Wang J, Qu K, Zhang J, Li L, et al. m6A RNA modification controls cell fate transition in mammalian embryonic stem cells. Cell Stem Cell 2014;15(6):707–19.
[14] Li Y, Wang X, Li C, Hu S, Yu J, Song S. Transcriptome-wide N6-methyladenosine profiling of rice callus and leaf reveals the presence of tissue-specific competitors involved in selective mRNA modification. RNA Biol 2014;11(9):1180–8.
[15] Yang Y, Hsu PJ, Chen Y-S, Yang Y-G. Dynamic transcriptomic m6A decoration: writers, erasers, readers and functions in RNA metabolism. Cell Res 2018;28(6):616–24.
[16] Knuckles P, Lence T, Haussmann IU, Jacob D, Kreim N, Carl SH, et al. Zc3h13/Flacc is required for adenosine methylation by bridging the mRNA-binding factor Rbm15/Spenito to the m6A machinery component Wtap/Fl (2) d. Genes Dev 2018;32(5–6):415–29.
[17] Miao R, Dai CC, Mei L, Xu J, Sun SW, Xing YL, et al. KIAA1429 regulates cell proliferation by targeting c-jun messenger RNA directly in gastric cancer. J Cell Physiol 2020;235(10):7420–32.
[18] Zhang C, Fu J, Zhou Y. A review in research progress concerning m6A methylation and immunoregulation. Front Immunol 2019;10:922.
[19] Meyer KD, Jaffrey SR. Rethinking m6A readers, writers, and erasers. Annu Rev Cell Dev Biol 2017;33:319.
[20] Zaccara S, Ries RJ, Jaffrey SR. Reading, writing and erasing mRNA methylation. Nat Rev Mol Cell Biol 2019;20(10):608–24.
[21] Lei H, He M, He X, Li G, Wang Y, Gao Y, et al. METTL3 induces bone marrow mesenchymal stem cells osteogenic differentiation and migration through facilitating M1 macrophage differentiation. Am J Tourism Res 2021;13(5):4376.
[22] Pan Zp, Wang B, Hou Dy, You Rl, Wang Xt, Xie Wh, et al. METTL3 mediates bone marrow mesenchymal stem cell adipogenesis to promote chemoresistance in acute myeloid leukaemia. FEBS open bio 2021;11(6):1659–72.

[23] Zhang M, Zhai Y, Zhang S, Dai X, Li Z. Roles of N6-Methyladenosine (m6A) in stem cell fate decisions and early embryonic development in mammals. Front Cell Dev Biol 2020;8:782.
[24] Vu LP, Pickering BF, Cheng Y, Zaccara S, Nguyen D, Minuesa G, et al. The N6-methyladenosine (m6A)-forming enzyme METTL3 controls myeloid differentiation of normal hematopoietic and leukemia cells. Nat Med 2017;23(11):1369–76.
[25] Wu Y, Xie L, Wang M, Xiong Q, Guo Y, Liang Y, et al. Mettl3-mediated m6A RNA methylation regulates the fate of bone marrow mesenchymal stem cells and osteoporosis. Nat Commun 2018;9(1):1–12.
[26] Liang Y, Han H, Xiong Q, Yang C, Wang L, Ma J, et al. METTL3-Mediated m6A methylation regulates muscle stem cells and muscle regeneration by notch signaling pathway. Stem Cell Int 2021;2021.
[27] Lu Z, Yan L, Pei M. Commentary on 'Surface markers associated with chondrogenic potential of human mesenchymal stromal/stem cells. 2020. F1000Research 9.
[28] Li M, Zha X, Wang S. The role of N6-methyladenosine mRNA in the tumor microenvironment. Biochim Biophys Acta, Rev Cancer 2021;1875(2):188522.
[29] Wang L, Hu L, Zhou X, Xiong Z, Zhang C, Shehada H, et al. Exosomes secreted by human adipose mesenchymal stem cells promote scarless cutaneous repair by regulating extracellular matrix remodelling. Sci Rep 2017;7(1):1–12.
[30] Chang C-H, Lin Y-L, Tyan Y-S, Chiu Y-H, Liang Y-H, Chen C-P, et al. Interleukin-1β-induced matrix metalloproteinase-3 via ERK1/2 pathway to promote mesenchymal stem cell migration. PLoS One 2021;16(5):e0252163.
[31] van Beuningen HM, de Vries-van Melle ML, Vitters EL, Schreurs W, van den Berg WB, van Osch GJ, et al. Inhibition of TAK1 and/or JAK can rescue impaired chondrogenic differentiation of human mesenchymal stem cells in osteoarthritis-like conditions. Tissue Eng 2014;20(15–16):2243–52.
[32] Kim YJ, Kim HK, Cho HH, Bae YC, Suh KT, Jung JS. Direct comparison of human mesenchymal stem cells derived from adipose tissues and bone marrow in mediating neovascularization in response to vascular ischemia. Cell Physiol Biochem 2007;20(6):867–76.
[33] Arai Y, Choi B, Kim BJ, Park S, Park H, Moon JJ, et al. Cryptic ligand on collagen matrix unveiled by MMP13 accelerates bone tissue regeneration via MMP13/Integrin α3/RUNX2 feedback loop. Acta Biomater 2021;125:219–30.
[34] Wang M, Sampson ER, Jin H, Li J, Ke QH, Im H-J, et al. MMP13 is a critical target gene during the progression of osteoarthritis. Arthritis Res Ther 2013;15(1):1–11.
[35] Zhang C, Tang W, Li Y. Matrix metalloproteinase 13 (MMP13) is a direct target of osteoblast-specific transcription factor osterix (Osx) in osteoblasts. PLoS One 2012;7(11):e50525.
[36] Ho I, Vorhees P, Marin N, Oakley BK, Tsai S-F, Orkin S, et al. Human GATA-3: a lineage-restricted transcription factor that regulates the expression of the T cell receptor alpha gene. EMBO J 1991;10(5):1187–92.
[37] Li Y, Zhong W, Huang Q, Lang B, Tang X. GATA3 improves the protective effects of bone marrow-derived mesenchymal stem cells against ischemic stroke induced injury by regulating autophagy through CREG. Brain Res Bull 2021;176:151–60.
[38] Ma L, Xue W, Ma X. GATA3 is downregulated in osteosarcoma and facilitates EMT as well as migration through regulation of slug. OncoTargets Ther 2018;11:7579.
[39] Kouros-Mehr H, Slorach EM, Sternlicht MD, Werb Z. GATA-3 maintains the differentiation of the luminal cell fate in the mammary gland. Cell 2006;127(5):1041–55.
[40] Sellheyer K, Krahl D. Expression pattern of GATA-3 in embryonic and fetal human skin suggests a role in epidermal and follicular morphogenesis. J Cutan Pathol 2010;37(3):357–61.